

# A Frequency Reference Photonic Integrated Circuit for WDM with Low Polarization Dependence

J.-M. Verdiell, M. A. Newkirk, T. L. Koch, R. P. Gnall, U. Koren, B. I. Miller, and B. Tell

**Abstract**—A photonic circuit implementing ten frequency reference filters for narrow-channel wavelength division multiplexing (WDM) has been fabricated. A diluted multi-quantum-well waveguide structure is shown to yield a very low TE/TM polarization dependence of 1 Å, as well as improved absolute frequency control and reproducibility. A standard deviation in absolute filter wavelength of 3.33 Å is measured on a random set of devices from a 2 in wafer. The ten channels are evenly spaced by 7.2 Å. Such filters can be used to lock tunable lasers to a set of reference frequencies for WDM applications. The demonstrated diluted multi-quantum-well waveguide structure with low birefringence and improved absolute wavelength control could potentially be used in other WDM integrated circuit requiring tight wavelength tolerance and polarization insensitivity.

WAVELENGTH division multiplexing (WDM) is attracting considerable interest in the field of fiber optic telecommunications. With the advent of all-optical fiber links using Er-doped amplifiers, WDM provides a way to upgrade existing links to higher capacity by transmitting different wavelength carriers in one fiber. Photonic integrated circuits (PIC's) based on semiconductor systems such as InGaAsP could play a major role in this new technology, since they could significantly lower the cost of the necessary tunable sources and wavelength mux/demux components compared to their bulk or fiber optic counterparts. However, with present PIC fabrication techniques, achieving absolute wavelength reproducibility on the order of a few angstroms, as would be required for dense WDM, is still a considerable challenge. Moreover, most of the components demonstrated up to now in InGaAsP have a nonnegligible polarization dependence, i.e., the center frequency of the wavelength sensitive elements shifts when the input light polarization rotates from TE to TM. In this letter, we show that low TE/TM sensitivity and improved wavelength reproducibility can be achieved using a properly designed multi-quantum-well (MQW) waveguide. We demonstrate the potential of such a waveguide structure in a PIC implementing a WDM reference filter for ten closely spaced frequencies.

The layout of the circuit is presented in Fig. 1. The purpose of the chip is to provide an electrical signal exhibiting a dip when the input light matches a specific

wavelength. It performs a function analogous to an absorption resonance in a gas, which is commonly used to lock tunable lasers to a specific reference frequency [1]. Apart from smaller size and ease of use, an advantage of this PIC over an atomic absorption line is that it can be designed for an arbitrary wavelength, or even multiple wavelength. For example, our single chip provides ten different wavelength channels with equal spacing.

The working principle is as follows. Light is launched into a 500 μm long rib loaded waveguide, then freely expands in the plane of a MQW slab waveguide for 2 mm. The expanding beam travels through a 3 mm long Bragg grating section (grating strength  $\kappa < 10 \text{ cm}^{-1}$ ), and is finally intercepted by an array of ten detectors, which sample the light coming out at different angles through the grating. Because each ray propagating at an angle  $\theta$  with respect to the grating vector sees a different effective grating pitch, the grating resonance wavelength  $\lambda(\theta)$  obeys the relation:

$$\frac{\lambda - \lambda_0}{\lambda_0} \approx \frac{n_{\text{eff}}}{n_{\text{eff group}}} (\cos \theta - 1) \quad (1)$$

where  $n_{\text{eff}}$  is the effective index of the MQW waveguide,  $n_{\text{eff group}}$  is the group index of the guide defined by  $n_{\text{eff group}} = n_{\text{eff}} - \lambda \partial n_{\text{eff}} / \partial \lambda$ , and the Bragg wavelength  $\lambda_0$  at  $\theta = 0$  is determined by the grating pitch  $\Lambda = \lambda_0 / 2n_{\text{eff}}$ . The ten channels were designed to be centered at  $\lambda_0 = 1.56 \text{ μm}$  with a spacing of 7.7 Å ( $\sim 95 \text{ GHz}$ ). The detector widths were varied from 22 to 12 μm in order to yield a similar width of the frequency resonance curve from channel to channel. This results in a signal level imbalance in favor of the wider detectors. To counteract this effect, we chose to slightly slant the grating by 6.25° and have the input waveguide directly facing the smallest detector. To further improve the coupling from the grating region to the detector region, a layer of quaternary material was also used as a one step mode converter in front of the detectors.

Special attention has been given to the design of the waveguide portion which comprises the grating filter. The electric field continuity equations show that low slab waveguide birefringence requires small discontinuities at the core/cladding interface. It is also advantageous to enlarge the size of the core. Furthermore, the wavelength reproducibility of integrated optical filters that rely on

Manuscript received December 18, 1992.

The authors are with AT & T Bell Laboratories, Holmdel, NJ 07733.  
IEEE Log Number 9208232.

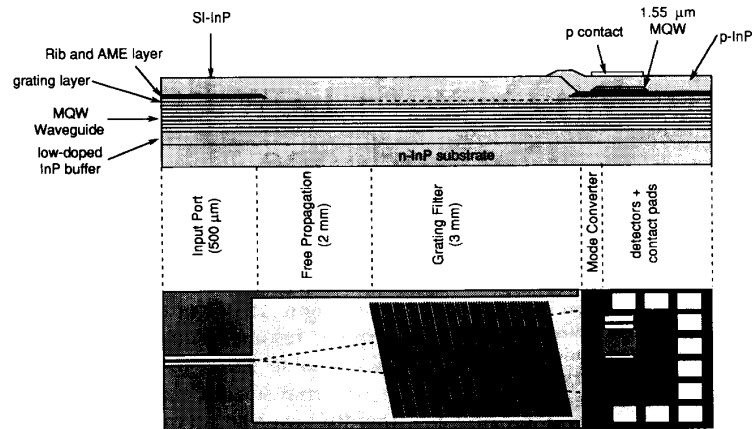


Fig. 1. Schematic drawing of the frequency reference PIC. Top: layer structure. Bottom: circuit layout.

geometrical dimensions of the structure (i.e., corrugation period and strength of a grating, phase-shift locations, relative facet locations, and physical length) is limited by the degree of control of the effective index of the waveguide, which is affected by the thickness of the waveguide layers and the material composition. For a change of thickness  $\Delta t$  and a change in material composition resulting in a  $\Delta\lambda_{pl}$  photoluminescence wavelength variation, the filter wavelength drift will be

$$\Delta\lambda = \frac{\lambda}{n_{eff\ group}} \left\{ \frac{\partial n_{eff}}{\partial t} \Delta t + \frac{\partial n_{eff}}{\partial \lambda_{pl}} \Delta \lambda_{pl} \right\}. \quad (2)$$

Since  $n_{eff}$  is confined between the cladding (usually InP) and the core index, minimizing the difference between these two indices by growing a core with a composition very close to InP will narrow the range of possible variations of  $n_{eff}$ . However, such quaternary materials are difficult to grow reproducibly. A better approach is to use a diluted multiquantum-well (MQW) core [2], [3], which consists of a few regularly spaced quantum-well separated by large binary material barriers. The MQW stack acts like an equivalent single layer [4] which index can be made arbitrarily close to that of InP, but does not require very tight composition control. Our waveguide core consists of nine 50 Å thick InGaAsP quantum wells ( $\lambda_{pl} = 1.10 \mu\text{m}$  in the bulk), separated by 1250 Å thick InP barriers. The bottom cladding is provided by the substrate and a low doped buffer layer of InP, while the upper cladding is a 1.2  $\mu\text{m}$  thick layer of semi-insulating Fe:InP. The theoretical performance of this MQW waveguide is compared in Fig. 2 with a standard laser waveguide (2000 Å core of  $\lambda_{pl} = 1.30 \mu\text{m}$  InGaAsP). A two-fold reduction in sensitivity versus material composition is expected, as well as an 8-fold reduction versus thickness errors. Most impressive is the 15-fold improvement for TE/TM sensitivity. Absolute numbers suggest that wavelength reproducibility down to a the Å level is readily achievable with present state of the art growth techniques. Those results

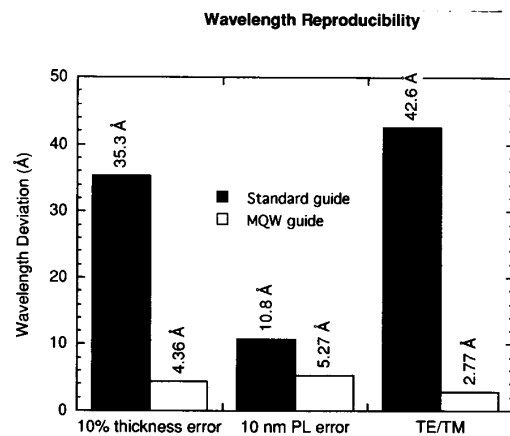


Fig. 2. Comparative wavelength variations and TE/TM sensitivity for a standard waveguide (left columns) and our diluted MQW waveguide (right columns).

were calculated using the transfer matrix method for evaluating the effective index of the waveguide and [5] for calculating the material index. No correction was applied to take into account the quantum effects in the wells.

We briefly describe the processing sequence of the PIC [6]. The base wafer before processing consisted of the MQW waveguide core just described, a 135 Å thick InGaAsP layer ( $\lambda_{pl} = 1.30 \mu\text{m}$ ), a 2000 Å thick InGaAsP layer ( $\lambda_{pl} = 1.30 \mu\text{m}$ ) which serves as the rib loading for the input guide and as a mode converter in front of the detectors, a stack of four InGaAs quantum wells with  $\lambda_{pl} = 1.30 \mu\text{m}$  barriers used for the detectors and absorbers, and finally p-doped InP layers. All the quaternary layers were separated by thin InP etch stops to facilitate processing. The InGaAs quantum wells were first removed by wet etching in the passive sections, and left to form the absorbers on each side of the chip and in a rectangle delimiting the detector region. Subsequent layers were patterned to form the input guide and the mode converter, then the grating was defined by holographic

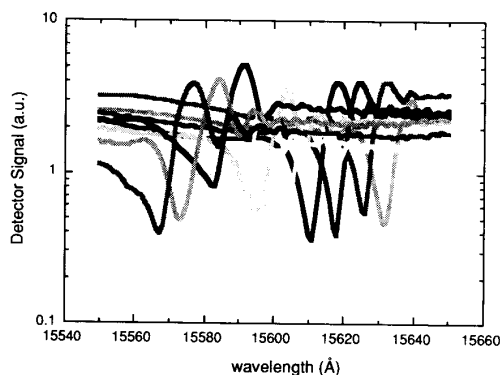


Fig. 3. Wavelength response of the ten channels.

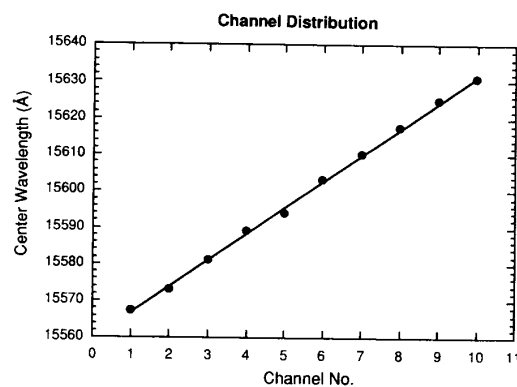
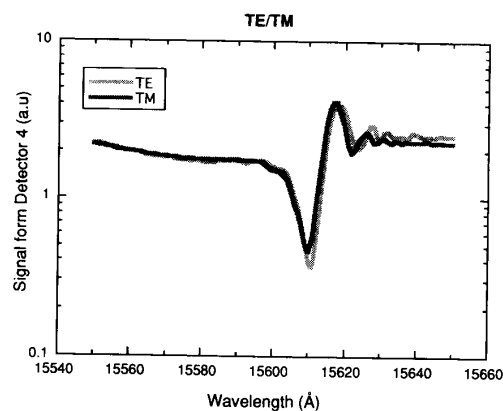


Fig. 4. Wavelength distribution of the ten channels.

exposure. The upper semi-insulating InP cladding layer was regrown, then selectively etched away over the detector and contact pad region.  $p^+$  doped contact layers were then regrown and etched away in the passive regions. After gold contact formation and patterning, the whole  $p^+$  region was ion implanted except for the detectors. A Cr/Au guard ring surrounding each detector and contact pad, not shown on the figure, was then deposited and patterned by liftoff. The total size of the cleaved device was  $6.1 \text{ mm} \times 1 \text{ mm}$ .

The device was tested using a HP tunable laser source coupled with a lensed fiber to the PIC. The polarization state was adjusted by monitoring the light coming from the back of the device using a Glan polarizer. Detector signal versus input wavelength is shown in Fig. 3 for the ten detectors. All channels exhibit a sharp dip at the prescribed resonance frequency, and also an overshoot on the longer wavelength side of the resonance. The cause of this apparent “ringing” on the longer wavelength side of the dip is not yet known. This behavior was observed in all the devices tested. The relative weakness of the grating insured that the dips were narrow enough (about  $7\text{--}8 \text{ \AA}$  FWHM) to be compatible with dense WDM channel spacing. The center wavelength of each channel is plotted in Fig. 4. Channels are very regularly spaced as assessed by the high correlation coefficient  $R = 0.999$  of the linear fit. A spacing of  $7.2 \text{ \AA}$  is measured, which is within  $0.5 \text{ \AA}$  of the design goal.

In order to assess the absolute wavelength reproducibility, we measured the first channel wavelength of 33 devices chosen randomly among two samples measuring about 1 square in each. These samples were processed separately but came from the same 2 in diameter base wafer. The standard deviation obtained from these measurements is  $\sigma = 3.33 \text{ \AA}$ , and the maximum range is  $12 \text{ \AA}$ . Although this represents a good result, we believe that these statistics may be limited by the unevenness of the grating layer, which was partially washed out during regrowth, and not by the uniformity of the MQW guide itself. This is substantiated by the observation that devices showing weaker grating responses have their frequency

Fig. 5. Filter response under TE and TM mode excitation. Wavelength shift is about  $1 \text{ \AA}$ . (this trace corresponds to channel 6).

response shifted towards shorter wavelength. The exact variation of the photoluminescence of the  $1.1 \mu\text{m}$  quantum wells across this particular wafer was not measured, but in the MOVPE growth system used for this wafer it is typically around  $10 \text{ nm}$ , with a standard deviation of  $4\text{--}5 \text{ nm}$ . From the aforementioned calculations, this should yield a filter reproducibility twice as good as the measured one.

Finally, we investigated the TE/TM sensitivity of the devices. Fig. 5 shows superimposed curves obtained for each polarization. The average wavelength shift was  $1 \text{ \AA}$ . One of the detectors (channel 10) showed the largest shift of  $2 \text{ \AA}$ . All other channels had shifts below  $1.2 \text{ \AA}$ . To the best of our knowledge, this represents the lowest polarization sensitivity ever reported for an InP-based PIC filter.

In conclusion, we have demonstrated that the use of diluted multiquantum-well waveguides can improve frequency reproducibility and TE/TM independence of WDM PIC's. Such a waveguide structure has been implemented in a PIC incorporating ten frequency reference channels for closely spaced WDM applications. Measured TE/TM sensitivity of  $1 \text{ \AA}$  and wavelength standard deviation of  $3.3 \text{ \AA}$  are reported. These results suggest that PIC

fabrication tolerances can match the requirements needed for future WDM systems.

#### REFERENCES

- [1] Y. C. Chung, R. M. Derosier, H. M. Presby, C. A. Burrus, Y. Akai, and M. Masuda, "A 1.5  $\mu\text{m}$  laser package frequency locked with a novel miniature discharge lamp," *IEEE Photon. Technol. Lett.*, vol. 3, pp. 841–844, 1991.
- [2] R. J. Deri, N. Yasuoka, M. Makiushi, A. Kuramata, and O. Wada, "Efficient fiber coupling to low loss diluted multiple quantum well optical waveguides," *Appl. Phys. Lett.*, vol. 55, pp. 1495–1497, 1989.
- [3] U. Koren, B. I. Miller, T. L. Koch, G. D. Boyd, R. J. Capik, and S. E. Socolich, "Low loss InGaAs/InP multiple quantum well waveguides," *Appl. Phys. Lett.*, vol. 49, pp. 1602–1603, 1986.
- [4] G. M. Alman, A. Molter, H. Shen, and M. Dutta, "Refractive index approximation from linear perturbation theory for planar MQW waveguides," *IEEE J. Quantum Electron.*, vol. 28, pp. 650–657, 1992.
- [5] C. H. Henry, L. F. Johnson, R. A. Logan, and D. P. Clarke, "Determination of the refractive index of InGaAsP epitaxial layers by mode line luminescence spectroscopy," *IEEE J. Quantum Electron.*, vol. QE-21, pp. 1887–1892, 1985.
- [6] T. L. Koch and U. Koren, "Semiconductor photonic integrated circuits," *IEEE J. Quantum Electron.*, vol. 27, pp. 641–653, 1991.

## Fabrication and Characterization of an In<sub>0.53</sub>Ga<sub>0.47</sub>As/InP Photon Transport Transistor

A. K. Chu, Y. Gigase, H. Y. Lee, M. J. Hafich, G. Robinson, and B. Van Zeghbroeck

**Abstract**—A photon transport transistor fabricated using the lattice-matched In<sub>0.53</sub>Ga<sub>0.47</sub>As/InP material system is reported. The device consists of a light emitting diode integrated on the top of a photodiode, with very tight optical coupling between the two devices. The device behaves like a bipolar junction transistor except that photons rather than minority carriers are transported through the base region. The device fabricated has a voltage gain of 258, a current gain of 0.07 yielding an electrical power gain of 18.1. The center wavelength emitted by the light emitting diode is at 1.55  $\mu\text{m}$ .

IN recent years, the development of optoelectronic integrated circuits (OEIC) has led to a very significant increase in both the operation speed of the circuits [1], [2] and the scale of integration [3], [4]. A survey of the literature [1]–[6] reveals that most OEIC's contain either a detector integrated with electronic circuits, as is typical for high-speed optoelectronic receiver circuits, or a light emitting device integrated with electronic circuits. Only few optoelectronic circuits have been reported [7], [8]

which integrate a light emitter with a detector and electronic circuits even though such circuits clearly have a larger functionality. In fact, such general purpose circuits are expected to be important for the next generation of optical communication and information processing systems.

The problems faced when fabricating such general purpose OEIC's are mainly due to their complex technology. Even when all devices can be readily fabricated on a single substrate, there are compositional and structural differences between photonic devices and electronic circuits which cause inherent tradeoffs among devices, while the fabrication of three different devices on the same substrate increases the number of process steps way beyond that of any electronic integrated circuit technology. It is the process complexity and the associated low yield which forms the major stumbling block towards general purpose OEIC's.

With this goal in mind, we have studied a novel optoelectronic device structure which can be used as a light source, a photodetector, and a transistor. The device consists of a light emitting diode structure which is monolithically integrated on top of a p-i-n photodiode. The combination of the two devices yields an electronic three-terminal device with gain. This device concept was pioneered in the early 1960's by Rediger *et al.* [9] and Ruth [10]. More recent work using the GaAs/AlGaAs material system yielded devices with a current gain up to 4, a voltage gain larger than 10 000 and a unity-gain frequency of 70 MHz [11]. We will refer to this device as the photon transport transistor (PTT) since photons are transported through the base region. This device is suitable for OEIC's

Manuscript received November 30, 1992; revised February 2, 1993. This work was supported by the National Science Foundation under Contract CDR 8622236.

A. K. Chu and B. Van Zeghbroeck are with the Department of Electrical and Computer Engineering and the Optoelectronic Computing System Center, University of Colorado at Boulder, Boulder, CO 80309.

H. Y. Lee, M. J. Hafich, and G. Robinson are with the Department of Electrical Engineering and the Optoelectronic Computing System Center, Colorado State University, Fort Collins, CO 80523.

Y. Gigase was with the Optoelectronic Computing System Center, Colorado State University, Fort Collins, CO 80523. He is currently with Alcatel in Antwerp, Belgium.

IEEE Log Number 9208239.